Discover Environment

Case Study

Estimation of tree attributes in mixed tropical hill forests using Landsat-8 and Sentinel-1 data

Ariful Khan[1] · Md. Shawkat Islam Sohel[2] · Md. Shamim Reza Saimun[1] · Mohammed Abu Sayed Arfin Khan[1] · M. Salim Uddin[3] · Melanie L. Harris[2] · Parvez Rana[4]

Received: 12 January 2025 / Accepted: 21 May 2025
Published online: 03 June 2025

Abstract
Estimating forest attributes is crucial for understanding forest performance. While forest protection and tree plantations can serve as cost-effective mitigation strategies to address climate change challenges, monitoring natural forests and plantations remains expensive and challenging for a developing nation like Bangladesh, which is highly donor-dependent and lacks advanced remote sensing research facilities such as LiDAR or drone technology. In this context, open-source remote sensing data can serve as an effective tool for monitoring forest structure. In this study, we evaluated the ability of Landsat-8 and Sentinel-1 data to predict forest attributes using ground-measured tree data from 110 plots (each 400 m^2 in size). We applied the random forest algorithm to predict tree height, density, basal area, and volume in two forest-protected areas of Bangladesh. For tree height and tree density, Sentinel-1 showed slightly higher prediction accuracy (RMSE = 7% and 46%, respectively) compared to Landsat-8 and combined data (Landsat-8 and Sentinel-1). Landsat-8 data had a higher prediction accuracy (RMSE = 23%) for basal area compared to Sentinel-1 and combined data. For volume, the combined dataset outperformed Sentinel-1 and Landsat-8; however, prediction accuracy was low. Our results indicate that height and basal area can be well predicted by combining Sentinel and Landsat data. The results underscore the value of open-source remote sensing tools as cost-effective alternatives for forest monitoring, offering critical insights for forest management and climate change mitigation strategies in developing nations.

Keywords Forest structure · Basal area · Tree density · Volume · Random forest algorithm

1 Introduction

Forests are integral to human existence, serving not only as a source of consumable goods but also providing vital ecosystem services that support our well-being, such as maintenance of ecological balance, preservation of environmental integrity, and enhancement of aesthetic value [51, 53]. To sustain these critical functions, effective forest management is imperative for both present and future generations [39, 44]. Key structural attributes like volume, basal area, and the number of trees per unit area are vital data points to enable efficient forest management.

✉ Parvez Rana, parvez.rana@luke.fi; Ariful Khan, md.arifk65@student.sust.edu; Md. Shawkat Islam Sohel, soheluq@gmail.com; msohel@usc.edu.au; Md. Shamim Reza Saimun, saimun-fes@sust.edu; Mohammed Abu Sayed Arfin Khan, khan-for@sust.edu; M. Salim Uddin, m-salim.uddin@uvm.edu; Melanie L. Harris, mharris3@usc.edu.au | [1]Department of Forestry and Environmental Science, Shahjalal University of Science and Technology, Sylhet, Bangladesh. [2]School of Science, Technology and Engineering and Forest Research Institute, University of the Sunshine Coast, Sippy Downs, Sunshine Coast, Australia. [3]Rubenstein School of Environment and Natural Resources, The University of Vermont, 81 Carrigan Drive, Burlington, VT 05405, USA. [4]Natural Resources Institute Finland (Luke), Latokartanonkaari 9, 00790 Helsinki, Finland.

These attributes offer valuable insights about the forest's composition and are instrumental in guiding sustainable practices for the preservation and utilization of this valuable natural resource [4, 13, 47].

Forest inventory, a systematic process involving the collection of field measurements and the application of statistical principles, forms the basis for obtaining forest structural attributes for assessing forest resources and planning management strategies, whether it is conducted at the national level or focused on individual stands (a management unit) or sample plots. These approaches serve as a foundation for making inferences about the forest's population. By leveraging statistical theory, forest inventory extrapolates findings from sampled plots to describe the characteristics and dynamics of whole forest landscapes. However, conducting traditional field surveys can be resource-intensive, time-consuming, and logistically difficult. Furthermore, non-response in these surveys might occur, where certain field plots are inaccessible, leading to limited sample sizes and potentially biased estimates [11, 31, 45].

Emerging technologies such as remotely sensed satellite imagery and machine learning offer promising alternatives to traditional forest inventory methods. Since the introduction of satellite imagery for forest inventory purposes in the 1950s, remote sensing systems have become integral tools in the field of forestry, aiding activities like forest cover monitoring, land use change assessment, and forest biomass estimation. Mapping forest structure across a vast region requires a comprehensive approach that integrates field-based measurements with data from both passive and active remote sensors, along with auxiliary information such as elevation [54], environmental factors, terrain-related data [49, 58], and geographic coordinates [29]. Utilizing auxiliary data from remote sensing has been proven to significantly enhance precision in forest inventory compared to traditional measurement methods. Remote sensing provides cost-effective proxies for modeling forest attributes, delivering accurate measurements over large areas and surpassing the limitations of traditional field inventories [6, 48]. Studies have demonstrated the considerable advancements in precision offered by remote sensing technologies [9, 35–37]. Furthermore, remote sensing provides a mechanism for deriving forest attribute maps that are valuable to forest managers. However, reliable and comprehensive maps of forest attributes are limited, particularly over large geographic areas, because they require an array of field data and reliable predictors [59].

Since the inception of the Landsat satellite in 1972, researchers have been actively leveraging data collected by satellite sensors to enhance estimations of forest structure. Successive satellite deployments with upgraded capabilities have resulted in improved image resolution, heightened temporal frequency of Earth's land surface monitoring, and expanded spectral coverage. These advancements have made multispectral satellite data invaluable for modeling and mapping crucial forest attributes across diverse landscapes [14]. Notably, fine-resolution optical satellite imagery emerges as particularly beneficial for accurately predicting forest structure [16, 57]. Studies by Abdollahi et al. [1], Goodbody et al. [15], Peña-Lara et al. [41], and Shamsoddini et al. [57] have underscored the efficacy of multispectral satellite data in this regard.

Microwave remote sensing has distinct advantages in continuous monitoring irrespective of weather conditions and collecting data consistently throughout the day and night. Microwave remote sensing uses both vertical–vertical (VV) and vertical-horizontal (VH) polarizations, increasing its versatility and allowing for comprehensive data collection across a variety of environmental scenarios [30]. VH, in particular, is highly sensitive to the dynamics of vegetation density and structure [24]. Integration of both optical and microwave remote sensing can gain comprehensive insights about the forest attributes. The combination of Sentinel-1 and −2 data, along with coordinates, were identified as the best predictors while developing a model for mapping forest structures, as noted by Silveira et al. [59]. However, predicting mixed forest ecosystem structures in tropical regions using Landsat and Sentinel data can be challenging due to several factors, including the complexity of tropical forest ecosystems, the limited spectral resolution of Landsat and Sentinel sensors, and the presence of dense vegetation cover [25].

Combining high quality remote sensing data with forest inventory data can improve the accuracy of estimations and provide more reliable spatial and temporal analyses [18, 61, 63]. In Bangladesh, research on predicting forest structures using remote sensing data has been limited due to constraints in research infrastructure and resources. However, despite these challenges, there is increasing recognition of the value of freely available remote sensing data for effective forest monitoring and management. This research is particularly significant for Bangladesh, where forests play a crucial role in biodiversity conservation, carbon sequestration, and climate change mitigation. By demonstrating the potential of freely available remote sensing data in estimating forest attributes with reasonable accuracy, this study may provide an affordable and scalable solution for forest monitoring, especially in resource-limited settings. The findings can support forest managers, conservationists, and policymakers in making informed decisions regarding sustainable forest management, afforestation programs, and biodiversity conservation efforts.

Additionally, since no study in Bangladesh has yet applied remote sensing to estimate forest attributes, the methodology presented in this study serves as a model for leveraging open-source remote sensing data to improve forest assessments. Therefore, this study integrates open-source Landsat-8 and Sentinel-1 data with random forest machine learning algorithm, a widely adopted approach known to estimate tropical forest attributes. Specifically, the objective of this study is to estimate key forest attributes, including tree height, density, basal area, and volume, using Sentinel-1 and Landsat-8 data.

2 Materials and methods

2.1 Study area

Our study was conducted in Khadimnagar National Park (KNP) and Rema-Kalenga Wildlife Sanctuary (RKWS), located in northeastern Bangladesh (Fig. 1). These areas represent some of the most biodiverse tropical forests in the country and are situated in regions of relatively high rainfall [28, 52].

KNP encompasses approximately 678.80 hectares of hilly terrain, positioned between 24°56′–24°58′ N latitude and 91°55′–91°59′ E longitude. In contrast, RKWS spans about 1796 hectares of tropical forest, located between 24°06′–24°14′ N latitude and 91°34′–91°41′ E longitude [8].

The annual average rainfall in KNP is 4045 mm, with July being the wettest month, averaging around 1250 mm of rainfall. December is the driest month, with almost no precipitation. The average maximum temperature in KNP is 28°C, while the average minimum is 17°C. RKWS experiences a moist tropical climate with heavy rainfall from May to October. The annual average rainfall in RKWS is 4162 mm, and the mean annual temperature is 24°C, with average maximum and minimum temperatures of 37°C and 27°C, respectively [32, 50].

The soils in KNP are moderately fertile, with generally low pH levels. Soil textures range from sandy loam to sandy clay loam [52]. In RKWS, soils vary from sandy loam to silty clay and are acidic in nature. The terrain is characterized by undulating slopes and hillocks, locally known as Tila, rising 10–50 m above the forest floor and scattered throughout the area. The Park is drained by numerous small, sandy-bedded streams [34].

2.2 Field data collection

During our field investigation in April 2021, we surveyed a total of 110 plots (20 m × 20 m). For every plot, the following information is gathered: diameter at breast height (DBH), crown width, elevation, species, and tree height. The starting measurement size was set at 5 cm in diameter. Each tree's diameter at breast height (DBH) was measured using a DBH tape. Tree height, as well as the crown widths in both the east–west and north–south directions, were measured using a laser rangefinder and a measuring tape. Basal area (BA) was calculated following Avery and Burkhart [2] using the formula: $BA = 0.00007854 \times DBH\,(cm)^2$

Tree density was determined by dividing the total number of trees (*N*) by the total sampled area (*A*), yielding the number of trees per hectare. Stem volume was estimated using DBH and tree height (h) with the formula: $V = \pi/4 \times d^2 \times h$, and the total stem volume per hectare was obtained by summing the volumes of all tree stems within each plot [3].

2.3 Remote sensing data

In order to download the remote sensing data, Google Earth Engine (GEE), a computing platform for geospatial analysis, was used in this study. Satellite images were retrieved for the months February-April from GEE. Landsat-8 Operational Land Imager (OLI) data was used. GEE provides access to 'Landsat-8 Level 2, Collection 2, Tier 1' dataset which contains atmospherically corrected surface reflectance data. An additional dataset used in this study through GEE was 'Sentinel-1 SAR GRD: C-band Synthetic Aperture Radar Ground Range Detected'. Images were retrieved from datasets utilizing the function *ee.ImageCollection* and.*filter*. The Landsat-8 satellite imagery used in this study was acquired from 01 February 2021 to 30 April 2021. We filtered out imagery with cloud coverage over 40%. For the filtered imagery, we conducted cloud, and cloud shadow masking. Cloud and cloud shadow masking was applied to these images, followed by composite image generation using mean function to create a three-month composite image. We used Quality Assessment pixels to mask clouds, and cloud shadows, from these images. Similarly, the Sentinel-1 image composite was also generated. However, Landsat-8 has a spatial resolution of 30 m, and Senitnel-1 has 10 m, but the inventory plot size was 20 m × 20

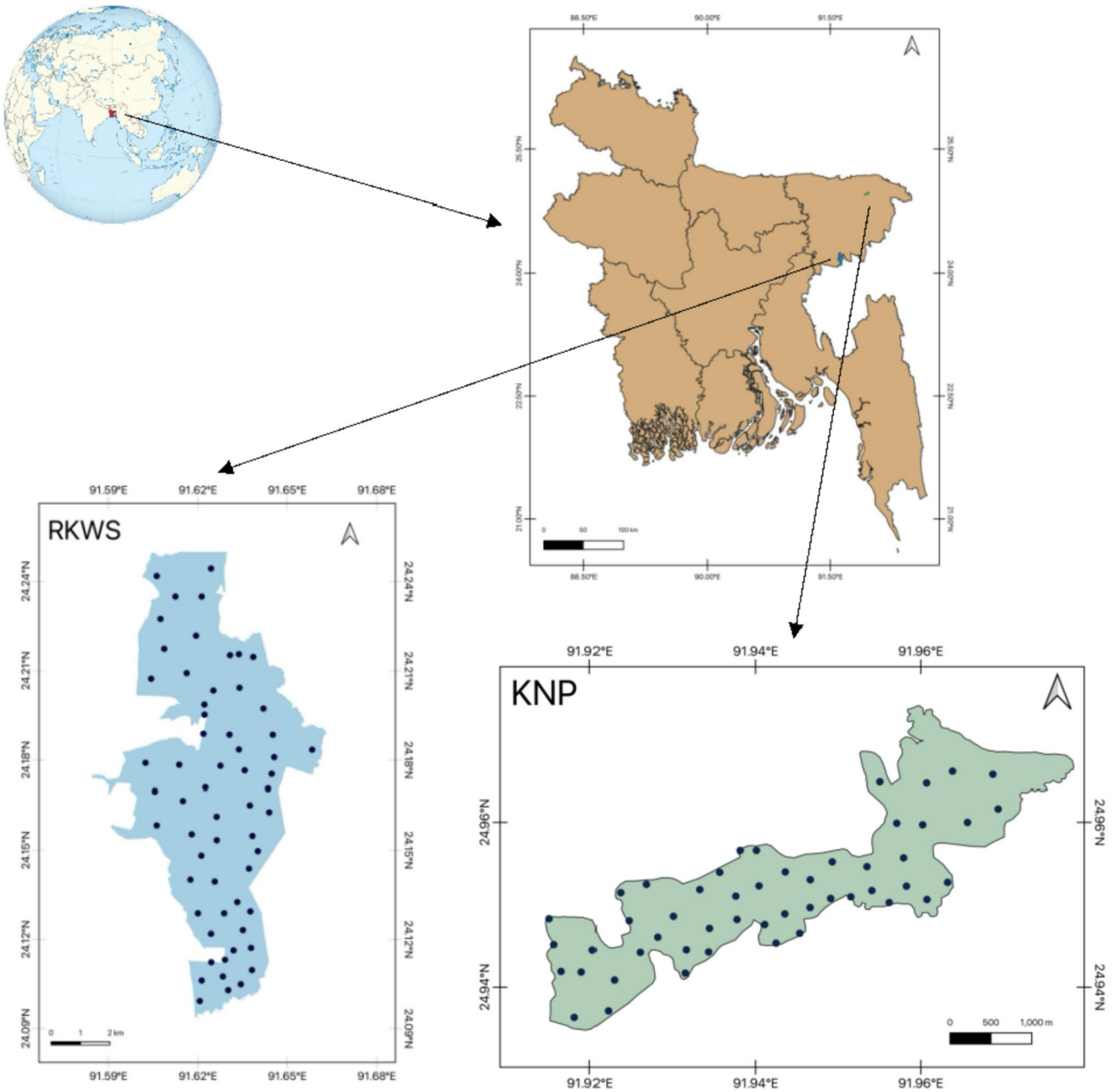

Fig. 1 Map of the study areas of *KNP* Khadimnagar National Park, and *RKWS* Rema-Kalenga Wildlife Sanctuary and their location within north-east region of Bangladesh

m. To address these issues, the average of adjacent pixels, also known as the neighborhood mean or focal mean, was used to estimate the central value. A 20 m buffer was generated around each inventory plot's center point, and the plot center location data were uploaded to a GEE asset and imported into the code editor. A function named 'buffer points' was used to create a square buffer. These buffer regions were then used to extract zonal statistics i.e., mean pixel value from raster datasets for each plot. In that case, Zonal statistics function was applied. Finally plot wise raster datasets predictor variables were exported as table for analysis (Table 1).

Remote sensing variables included surface reflectance data of individual Landsat-8 bands, Sentinel-1 bands (VH and VV), six vegetation indices i.e., ARVI (Atmospherically Resistant Vegetation Index), EVI (Enhanced Vegetation Index), GDVI (Green Difference Vegetation Index), GRVI (Green Ratio Vegetation Index), NDVI (Normalized Difference Vegetation Index), SAVI (Soil Adjusted Vegetation Index) generated using Landsat image, 1 band ratio i.e., VH/VV for Sentinel-1 image. All these variables were calculated in GEE. In addition, texture images were calculated applying grey-level co-occurrence

Table 1 List of remote sensing variables used in this study

Variable type (#)	Variable name	Description
Landsat-8 Surface Reflectance (6)	SR_B2, SR_B3, SR_B4, SR_B5, SR_B6, SR_B7	Landsat 8 bands- Blue, Green, Red, NIR, SWIR1, SWIR2
Landsat-8 Vegetation Index (6)	ARVI, EVI, GDVI, GRVI, NDVI, SAVI	Atmospherically Resistant Vegetation Index, Enhanced Vegetation Index, Green difference Vegetation Index, Green Ratio Vegetation Index, Normalized Difference Vegetation Index, Soil Adjusted Vegetation Index
Landsat-8 Texture (102)	SR_B*_asm, SR_B*_contrast, SR_B*_corr, SR_B*_var, SR_B*_idm, SR_B*_savg, SR_B*_svar, SR_B*_sent, SR_B*_ent, SR_B*_dvar, SR_B*_dent, SR_B*_imcorr1, SR_B*_imcorr2, SR_B*_diss, SR_B*_inertia, SR_B*_shade, SR_B*_prom	Landsat bands 2–7 texture analysis using grey-level co-occurrence matrix
Sentinel-1 Backscatter (2)	VV, VH	Sentinel-1 dual polarization backscatter
Sentinel-1 Band Ratio (1)	VH/VV	Band ratio of Sentinel-1
Sentinel-1 Texture (34)	V*_asm, V*_contrast, V*_corr, V*_var, V*_idm, V*_savg, V*_svar, V*_sent, V*_ent, V*_dvar, V*_dent, V*_imcorr1, V*_imcorr2, V*_diss, V*_inertia, V*_shade, V*_prom	Sentinel-1 texture analysis using grey-level co-occurrence matrix

SR_B*_xxx represents a texture image of individual Landsat-8 bands, where xxx is asm (Angular Second Moment), contrast (Contrast), corr (Correlation), var (Variance), idm (Inverse Difference Moment), savg (Sum Average), svar (Sum Variance), sent (Sum Entropy), ent (Entropy), dvar (Difference Variance), dent (Difference Entropy), imcorr1 (Information Measure of Corr.1), imcorr2 (Information Measure of Corr.2), diss (Dissimilarity), inertia (Inertia), shade (Cluster Shade), prom (Cluster prominence). V*_xxx represents a texture image of the individual Sentinel-1 bands where * is either V or H

matrix with a kernel size of 5 × 5 using *glcmTexture* function in GEE for both Landsat and Sentinel image. This produced 108 variables for Landsat and 36 for Sentinel images. These variables layers were then concatenated and *zonalStats* function was applied to extract the value of each plot.

2.4 Regression model for forest attributes prediction

A correlation filter was used to minimize multicollinearity among the predictors by excluding variables with a correlation value greater than 0.80. For each model, variables were introduced sequentially starting with the variable that exhibited the strongest correlation. This continued until further additions were not significant, or did not substantially improve model precision. For each model run, root mean square error (RMSE) values were examined prior to a variable addition [23, 38]. We employed random forest regressions to predict forest attributes, utilizing spectral bands and indices as predictor variables, with forest attributes as the response variable. We adopted the default parameter settings: 501 trees (*ntree*) and one-third of variables tried at each split (*mtry*). These default values have been proven adequate for remote sensing data [22, 45]. All statistical analysis was undertaken using R program [42]. We used R packages such as "*rcmdr. kmggplot*" for density plot, "*corrplot*" for correlation matrix and "*randomForest*" for prediction the models. The whole datasets were divided into training data and test data where 70% data were used for calibration and the remaining 30% data were used for validation of the model. The reliability of estimates was measured by root mean square error (RMSE) and mean difference (MD) [7, 33].

$$RMSE = \sqrt{\frac{1}{n}\sum_{i=1}^{n}(y_i - \hat{y}_i)^2} \tag{1}$$

$$RMSE\% = 100 * \frac{RMSE}{\bar{y}} \tag{2}$$

$$MD = \frac{1}{n}\sum_{i=1}^{n}(yi - \hat{y}i) \tag{3}$$

$$MD\% = 100 * \frac{MD}{\bar{y}} \tag{4}$$

Where, *yi* represents the observed value for a specific sample plot and $\hat{y}i$ represents the estimated value for the same sample plot *i*,$\bar{y}$ is the average value of measured sample plots, and n signifies the total count of sample plots.

3 Results

3.1 Forest attributes descriptive statistics

In KNP, the descriptive statistics revealed a range for height, stand volume, basal area, and tree density of 13 – 19 m, 21 – 972 m^3/ha, 3 – 5 m^2/ha, and 150 – 850 n/ha, respectively (Fig. 2a, b, c and d). In contrast, for RKWS, the descriptive statistics indicated a range for stand height, stand volume, basal area, and tree density of 12 – 16 m, 105 – 1916 m^3/ha, 2 – 11 m^2/ha, and 50 – 1200 n/ha, respectively (Fig. 2a, b, c and d).

3.2 Relationship between forest attributes and remote sensing predictors

Landsat-8 (n = 8, Fig. 3a) and Sentinel-1 (n = 7, Fig. 3b) predictors demonstrated statistically significant correlations with forest attributes, including height, tree density, basal area (BA), and volume. For Landsat, basal area showed a weak positive correlation (r = 0.21) with the EVI band, but negative correlations with other bands, particularly a weak negative correlation (r = – 0.22) with SR_B5. Similarly, height and volume were positively correlated (r = 0.04,

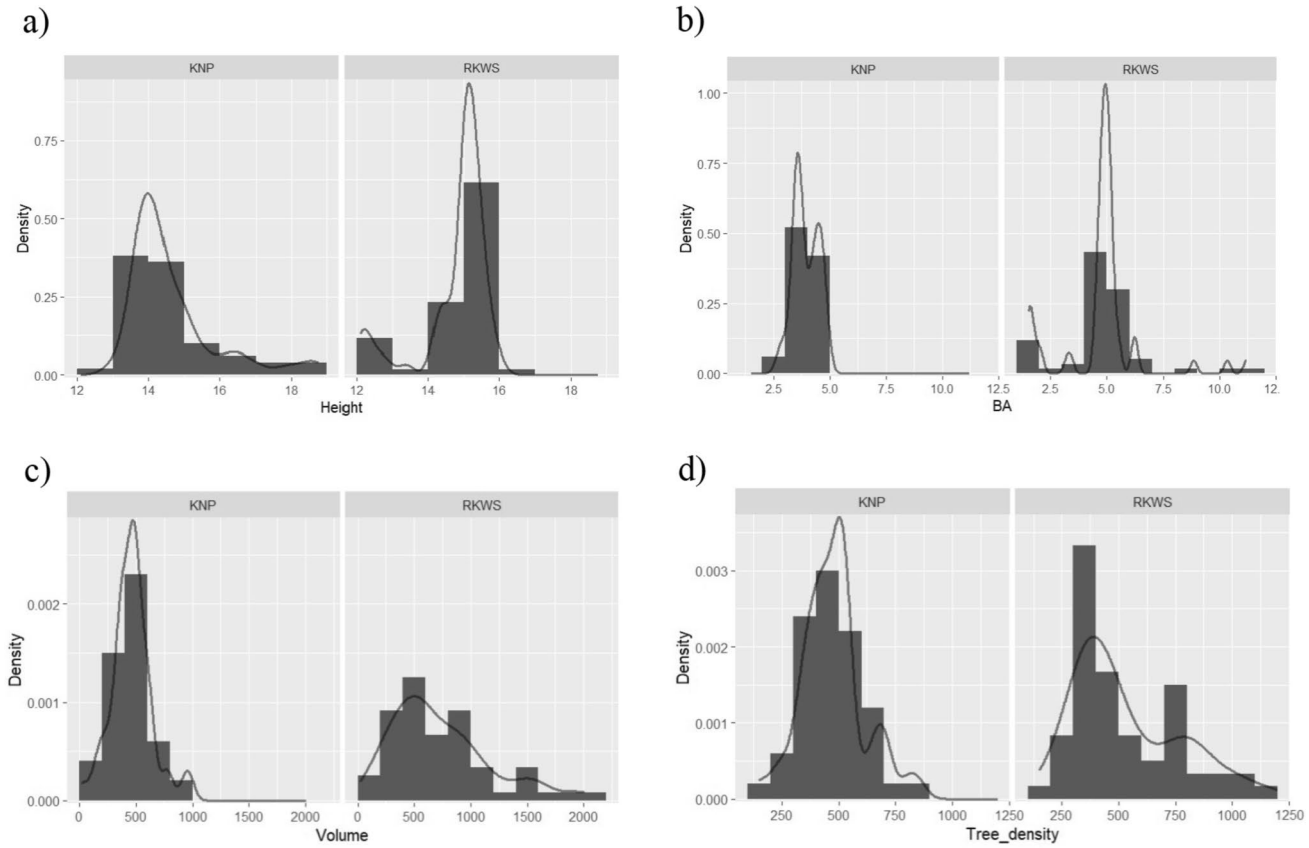

Fig. 2 Density curve with forest attributes (**a**) height, (**b**) basal area (BA), (**c**) volume and (**d**) tree density

r = 0.15) with EVI, but negatively correlated with other bands. Volume exhibited a negative correlation (r = − 0.31) with SR_B5. Conversely, tree density positively correlated (r = 0.06, r = 0.03) with EVI and ARVI, but negatively with other bands, particularly showing a weak negative correlation (r = − 0.12) with SR_B3.

In Sentinel-1 data, basal area and height exhibited weak positive correlations (r = 0.18, r = 0.22) with VH, while volume and tree density had weak positive correlations with VH/VV (r = 0.30, r = 0.15). However, they displayed negative correlations (r = − 0.17 with VH_dent, r = − 0.12 with VH_dvar).

3.3 Predicting forest attributes by remote sensing data

A comparative analysis of the performance of Landsat-8, Sentinel-1, and their combined datasets for predicting forest metrics, including height, basal area, tree density, and volume, indicates that Sentinel-1 consistently demonstrates slightly superior accuracy compared to Landsat-8 in predicting height and tree density (Table 2). Specifically, for height prediction, Sentinel-1 exhibits the lowest values (RMSE = 1.01, RMSE% = 6.82), whereas Landsat-8 displays higher error metrics (RMSE = 1.14, RMSE% = 7.68) and the combined dataset results in marginally higher errors (RMSE = 1.15, RMSE% = 7.76). Notably, Sentinel-1 (MD = 0.28, MD% = 1.19) are slightly higher than those for the combined dataset (MD = 0.20, MD% = 1.38) and Landsat-8 (MD = 0.17, MD% = 1.18) (Table 2). This suggests that while Sentinel-1 demonstrates superior overall accuracy, Landsat-8 displays slightly reduced error in terms of mean difference.

For tree density predictions, Sentinel-1 also exhibits enhanced performance, yielding lower RMSE values (RMSE = 241.88, RMSE% = 45.80) in comparison to Landsat 8 (RMSE = 259.52, RMSE% = 49.13) and the combined dataset (RMSE = 243.61, RMSE% = 25.54). However, Landsat-8 records a higher mean difference (MD = 48.28, MD% = 9.14) in contrast to the combined dataset values (MD = 29.81, MD% = 5.64) and Sentinel-1's values (MD = 37.89, MD% = 5.64) (Table 2).

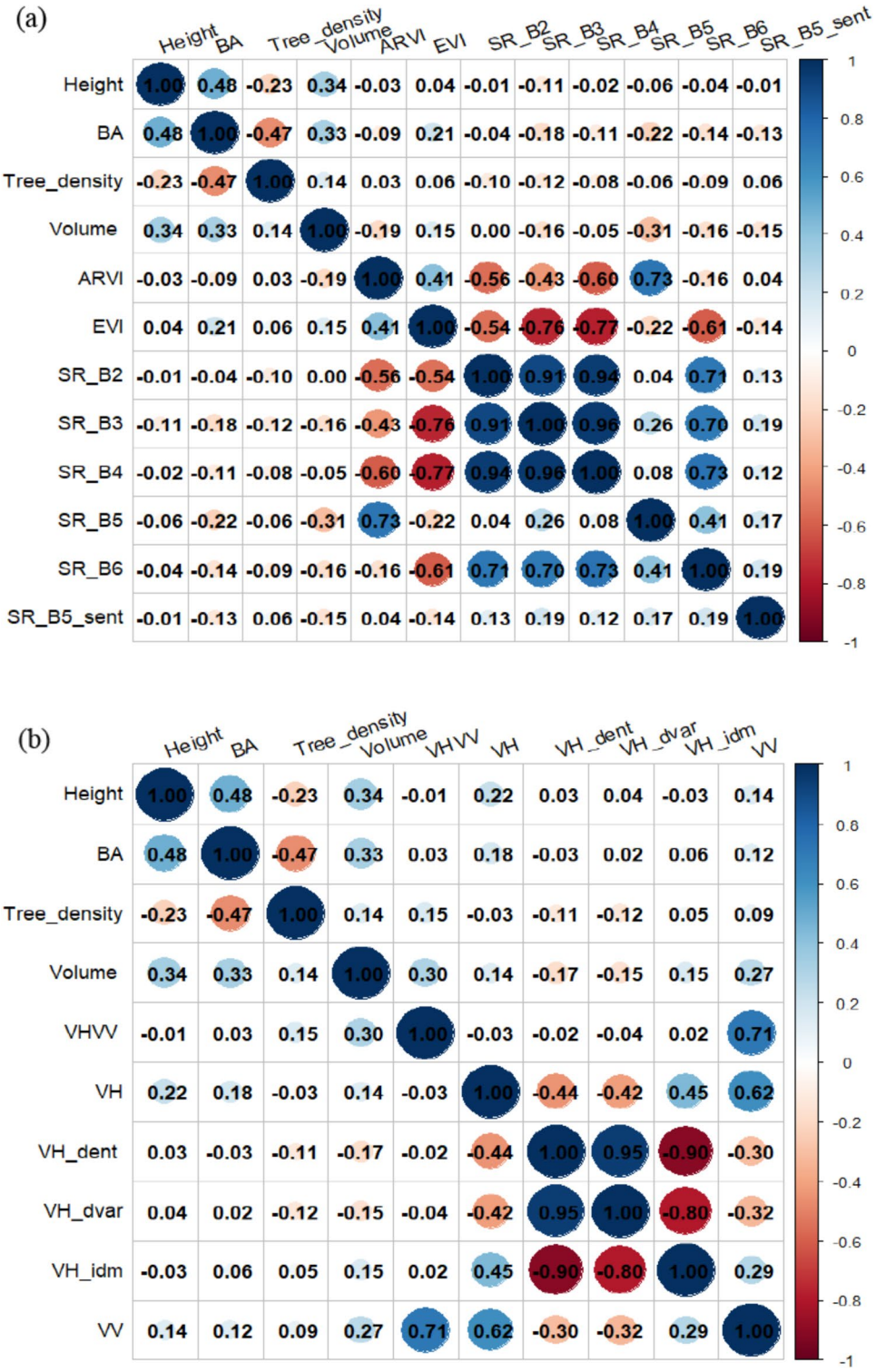

Fig. 3 Correlation coefficient (r) matrix (**a**) between DBH, BA, height, volume, tree density and Landsat-8 variables; (**b**) between BA, height, volume, tree density and sentinel-1 variables

Conversely, for the predictions of basal area and volume, Landsat-8 outperforms Sentinel-1, as evidenced by lower values of RMSE, RMSE%, MD, and MD%. Specifically, in basal area prediction, Landsat-8 achieves lower metrics (RMSE = 1.02, RMSE% = 23.09, MD = 0.22, MD% = 5.01), while the combined dataset and Sentinel-1 present higher error values (RMSE = 1.13, RMSE% = 25.54, and RMSE = 1.22, RMSE% = 27.52, respectively). Nonetheless, Sentinel-1 achieves a lower mean difference (MD) and mean difference percentage (MD%) of 0.12 and 7.79, respectively, compared to the combined dataset (MD = 0.19, MD% = 4.39) and Landsat-8 (MD = 0.22, MD% = 5.01) (Table 2). Thus, Landsat-8 demonstrates more

Table 2 Model performance using Landsat-8 (L) and Sentinel-1 (S) data

Forest attributes	RMSE			RMSE%			MD			MD%		
	L	S	L + S	L	S	L + S	L	S	L + S	L	S	L + S
Height	1.14	1.01	1.15	7.68	6.82	7.76	0.17	0.28	0.20	1.18	1.89	1.38
Tree density	259.52	241.88	243.61	49.13	45.80	46.12	48.28	37.89	29.81	9.14	7.17	5.64
Basal area	1.02	1.22	1.13	23.09	27.52	25.54	0.22	0.12	0.19	5.01	2.79	4.39
Volume	336.23	338.20	331.80	56.63	56.96	55.88	−16.88	−18.93	19.06	−2.84	−3.19	3.21

Landsat-8 variables were: EVI + ARVI + SR_B2 + SR_B3 + SR_B4 + SR_B5 + SR_B6 + SR_B5_sent;

Sentinel-1 variables were: VH/VV + VH_idm + VH_dvar + VH_dent + VV + VH;

Landsat-8 + Sentinel-1 variables were VH/VV + VH + ARVI + EVI + SR_B5 + SR_B5_sent

The abbreviation of the remote sensing variable can be found in Table 1

consistent estimates despite minor deviations. For volume predictions, the combined dataset (Landsat-8 + Sentinel-1) also shows improved performance with lower RMSE values (RMSE = 331.20, RMSE% = 55.88) compared to Landsat-8 (RMSE = 336.23, RMSE% = 56.63) and Sentinel-1 (RMSE = 338.20, RMSE% = 56.96). However, the combined dataset presents higher positive mean difference values (MD = 19.06, MD% = 3.21) compared to Landsat-8 (MD = −16.88, MD% = −2.84) and Sentinel-1 (MD = −18.93, MD% = −3.19) (Table 2).

4 Discussion

The comparison of Landsat-8, Sentinel-1, and combined Landsat-8 and Sentinel-1 datasets for predicting key forest attributes height, basal area, tree density, and volume demonstrates that the performance of remote sensing data varies depending on the specific forest attributes being predicted. Our findings align with previous research that highlights the strengths of different remote sensing data in estimating forest attributes, suggesting that the integration of optical (Landsat-8) and radar (Sentinel-1) data can enhance the accuracy of forest structure predictions [10, 12].

Our results indicate that Sentinel-1 outperforms Landsat-8 in predicting height and tree density, as evidenced by lower RMSE compared to Landsat-8 and the combined (Landsat-8 and Sentinel-1) datasets, indicating better overall accuracy. These findings are consistent with studies that have demonstrated the capability of radar-based data, such as Sentinel-1, to capture structural variations in forests due to its sensitivity to canopy height and volume [20, 55, 56, 59]. Although Landsat-8 exhibits slightly lower mean difference (MD) in predicting height compared to Sentinel-1 and the combined dataset, this suggests that while Sentinel-1 provides a more accurate overall estimate, Landsat-8's predictions deviate less from the mean. This indicates that Landsat-8 may offer more stable but less precise predictions [19]. Conversely, Landsat-8 displays higher MD in tree density predictions compared to Sentinel-1 and the combined dataset, reflecting greater error variance in its predictions [12]. In contrast, basal area predictions favored Landsat-8, as evidenced by lower RMSE, and MD values compared to Sentinel-1 and the combined dataset. The broader spectral bands of the optical sensor likely capture more detailed information on vegetation cover and biomass, making Landsat-8 more effective in assessing these attributes [62]. Similarly, for volume prediction, both datasets showed marginally improved performance with lower RMSE compared to Landsat-8 and Sentinel-1 alone. This suggests that while the combination of datasets reduces overall error in volume prediction, it may increase the likelihood of overestimating volume. This phenomenon has been observed in previous studies, where the combination of optical and radar data sometimes introduces complexities that lead to increased variance in predictions [43, 60].

Recent investigations underscore the potential of advanced methodologies, such as machine learning algorithms [21], and the integration of LiDAR data for enhancing predictions of forest attributes. Similarly, airborne laser scanning (ALS) has gained considerable traction for spatially quantifying variations in tree height and forest structure across diverse resolutions and forest types [5, 17, 27, 37, 40, 45]. The application of LiDAR surveys has become standard practice for stand-wise forest inventories in numerous countries [36, 46] and constitutes an integral component of various national forest inventory initiatives. However, LiDAR technology is quite expensive to afford by the forest department of Bangladesh because of limited funding support from the government. Future research should incorporate other available Synthetic Aperture Radar (SAR) data alongside Sentinel-1 and multispectral imagery for landscape-scale forest attribute studies, as these datasets are relatively inexpensive and, in some cases, open-source compared to LiDAR. SAR data from satellites

such as ALOS-2 PALSAR-2, NISAR, and RADARSAT-2/RCM provide valuable insights for studying forest attributes. ALOS-2 PALSAR-2, with its L-band SAR, is particularly useful for forest structure analysis, with some datasets freely available through JAXA [26]. The upcoming NISAR mission will offer open-access L- and S-band SAR data, enabling high-resolution monitoring of vegetation structure dynamics. Meanwhile, RADARSAT-2 and the RADARSAT Constellation Mission (RCM) provide C-band SAR data can also be utilized. Combining these SAR datasets with RapidEye, PlanetScope, and Sentinel-2 imagery can enhance forest attribute prediction at a large scale, particularly in regions with persistent cloud cover.

5 Conclusion

This study demonstrates the potential of open-source remote sensing data, specifically Landsat-8 and Sentinel-1, for estimating key forest attributes in resource-constrained settings such as Bangladesh. Sentinel-1 data exhibited slightly better performance in predicting tree height and density, while Landsat-8 data showed higher accuracy for basal area estimation. The combined use of Landsat-8 and Sentinel-1 data improved volume predictions, although accuracy remained relatively low. These findings highlight the complementary strengths of Sentinel-1 and Landsat-8 in monitoring forest structure, particularly in regions lacking advanced remote sensing technologies. The results underscore the value of open-source remote sensing tools as cost-effective alternatives for forest monitoring, offering critical insights for forest management and climate change mitigation strategies in developing nations. Future research could focus on refining predictive models and integrating additional data sources to further enhance accuracy and applicability in diverse forest ecosystems.

Acknowledgements We thank the Department of Forestry and Environmental Science, Shahjalal University of Science and Technology for providing lab and instruments support.

Author contributions AK and MASAK conceptualized and designed the study; AK and MASAK collected inventory data; MSRS and MSIS extracted remote sensing data; PR and MSIS analyzed the data; PR and MSIS supervised the study; AK wrote the paper and all the authors edited and reviewed the paper.

Funding Open access funding provided by Natural Resources Institute Finland. The first author Ariful Khan was supported by the National Science and Technology (NST) fellowship 2020/21. No additional funds, grants, or other financial support were received for this study.

Data availability Data are available from the corresponding author.

Declarations

Ethics approval and consent to participate Permission was obtained to conduct the field survey, and all procedures complied with national and institutional guidelines.

Consent for publication Not applicable.

Competing interests The authors declare no competing interests.

References

1. Abdollahi A, Yebra M. Forest fuel type classification: review of remote sensing techniques, constraints and future trends. J Environ Manage. 2023;342:118315. https://doi.org/10.1016/j.jenvman.2023.118315.
2. Avery TE, Burkhart HE. Forest Measurements. 5th ed. Boston: McGraw-Hill Series in Forest Resources, McGraw-Hill; 2002.
3. Avery TE, Burkhart HE. Forest measurements. Long Grove: Waveland Press; 2015.

4. Atkins JW, Bhatt P, Carrasco L, Francis E, Garabedian JE, Hakkenberg CR, Krause K. Integrating forest structural diversity measurement into ecological research. Ecosphere. 2023;14(9): e4633. https://doi.org/10.1002/ecs2.4633.
5. Buchelt A, Adrowitzer A, Kieseberg P, Gollob C, Nothdurft A, Eresheim S, Holzinger A. Exploring artificial intelligence for applications of drones in forest ecology and management. For Ecol Manage. 2024;551:121530. https://doi.org/10.1016/j.foreco.2023.121530.
6. Bouvier M, Durrieu S, Fournier RA, Renaud JP. Generalizing predictive models of forest inventory attributes using an area-based approach with airborne LiDAR data. Remote Sens Environ. 2015;156:322–34. https://doi.org/10.1016/j.rse.2014.10.004.
7. Cao L, Liu H, Fu X, Zhang Z, Shen X, Ruan H. Comparison of UAV LiDAR and digital aerial photogrammetry point clouds for estimating forest structural attributes in subtropical planted forests. Forests. 2019;10(2):145. https://doi.org/10.3390/f10020145.
8. Chowdhury MSH, Koike M. An overview on the protected area system for forest conservation in Bangladesh. J For Res. 2010;21:111–8. https://doi.org/10.1007/s11676-010-0019-x.
9. Dash JP, Marshall HM, Rawley B. Methods for estimating multivariate stand yield and errors using k-NN and aerial laser scanning. Forestry. 2015;88:237–47. https://doi.org/10.1093/forestry/cpu054.
10. Fang G, Xu H, Yang SI, Lou X, Fang L. Synergistic use of Sentinel-1, Sentinel-2, and Landsat 8 in predicting forest variables. Ecol Ind. 2023;151:110296. https://doi.org/10.1016/j.ecolind.2023.110296.
11. Fassnacht FE, Hartig F, Latifi H, Berger C, Hernández J, Corvalán P, Koch B. Importance of sample size, data type and prediction method for remote sensing-based estimations of aboveground forest biomass. Remote Sens Environ. 2014;154:102–14. https://doi.org/10.1016/j.rse.2014.07.028.
12. Fassnacht FE, Latifi H, Stereńczak K, Modzelewska A, Lefsky M, Waser LT, Ghosh A. Review of studies on tree species classification from remotely sensed data. Remote Sens Environ. 2016;186:64–87. https://doi.org/10.1016/j.rse.2016.08.013.
13. Gebreslasie MT, Ahmed FB, Van Aardt JA. Predicting forest structural attributes using ancillary data and ASTER satellite data. Int J Appl Earth Obs Geoinf. 2010;12:S23–6. https://doi.org/10.1016/j.jag.2009.11.006.
14. Gómez C, Alejandro P, Hermosilla T, Montes F, Pascual C, Ruiz Fernández LÁ, Valbuena R. Remote sensing for the Spanish forests in the 21st century: a review of advances, needs, and opportunities. For Syst. 2019;28(1):1–33. https://doi.org/10.5424/fs/2019281-14221.
15. Goodbody TR, Tompalski P, Coops NC, Hopkinson C, Treitz P, van Ewijk K. Forest inventory and diversity attribute modelling using structural and intensity metrics from multi-spectral airborne laser scanning data. Remote Sens. 2020;12(13):2109. https://doi.org/10.3390/rs12132109.
16. Hanna L, Tinkham WT, Battaglia MA, Vogeler JC, Ritter SM, Hoffman CM. Characterizing heterogeneous forest structure in ponderosa pine forests via UAS-derived structure from motion. Environ Monit Assess. 2024;196(6):530. https://doi.org/10.1007/s10661-024-12703-1.
17. Holmgren J, Nilsson M, Olsson H. Estimation of tree height and stem volume on plots using airborne laser scanning. For Sci. 2003;49:419–28. https://doi.org/10.1093/forestscience/49.3.419.
18. Hou Z, Mehtätalo L, McRoberts RE, Ståhl G, Tokola T, Rana P, Siipilehto J, Xu Q. Remote sensing-assisted data assimilation and simultaneous inference for forest inventory. Remote Sens Environ. 2019;234:111431.
19. Huang X, Ziniti B, Torbick N, Ducey MJ. Assessment of forest above ground biomass estimation using multi-temporal C-band Sentinel-1 and Polarimetric L-band PALSAR-2 data. Remote Sens. 2018;10(9):1424. https://doi.org/10.3390/rs10091424.
20. Joshi NP, Mitchard ET, Schumacher J, Johannsen VK, Saatchi S, Fensholt R. L-band SAR backscatter related to forest cover, height and aboveground biomass at multiple spatial scales across Denmark. Remote Sens. 2015;7(4):4442–72. https://doi.org/10.3390/rs70404442.
21. Jucker T, Caspersen J, Chave J, Antin C, Barbier N, Bongers F, Coomes DA. A regional model of canopy nonstructural carbohydrate distribution, carbon supply, and demand during drought. Glob Change Biol. 2019;25(10):3605–19.
22. Keränen K, Isoaho A, Räsänen A, Hjort J, Kumpula T, Korpelainen P, Rana P. Multi-resolution remote sensing for flark area detection in boreal aapa mires. Int J Remote Sens. 2024;45(13):4324–43. https://doi.org/10.1080/01431161.2024.2359732.
23. Latifi H, Fassnacht FE, Hartig F, Berger C, Hernández J, Corvalán P, Koch B. Stratified Aboveground Forest Biomass Estimation by Remote Sensing Data. Int J Appl Earth Obs Geoinf. 2015;38:229–41. https://doi.org/10.1016/j.jag.2015.01.016.
24. Liu Y, Gong W, Xing Y, Hu X, Gong J. Estimation of the forest stand mean height and aboveground biomass in Northeast China using SAR Sentinel-1B, multispectral Sentinel-2A, and DEM imagery. ISPRS J Photogramm Remote Sens. 2019;151:277–89. https://doi.org/10.1016/j.isprsjprs.2019.03.016.
25. Lu D. The potential and challenge of remote sensing-based biomass estimation. Int J Remote Sens. 2006;27:1297–328. https://doi.org/10.1080/01431160500486732.
26. Lucas R, Clewley D, Rosenqvist Å, Kellndorfer J, Walker W, Hoekman D, Shimada M, de Navarro Mesquita H. Global forest monitoring with synthetic aperture radar (SAR) data. In: Lunetta RS, Lyon JG, editors. Remote sensing and GIS accuracy assessment. Boca Raton: CRC Press; 2014. p. 295–322. https://doi.org/10.1201/b13040-15.
27. Maltamo M, Eerika ¨inen K, Packale´n P, Hyyppa ¨ J. Estimation of stem volume using laser scanning-based canopy height metrics. Forestry. 2006;79:217–29. https://doi.org/10.1093/forestry/cpl007.
28. Masum KM, Hasan MM. Assessment of land cover changes from protected forest areas of Satchari National Park in Bangladesh and implications for conservation. J For Environ Sci. 2020;36(3):199–206. https://doi.org/10.7747/JFES.2020.36.3.199.
29. Matasci G, Hermosilla T, Wulder MA, White JC, Coops NC, Hobart GW, Zald HS. Large-area mapping of Canadian boreal forest cover, height, biomass and other structural attributes using Landsat composites and lidar plots. Remote Sens Environ. 2018;209:90–106. https://doi.org/10.1016/j.rse.2017.12.020.
30. Mavrovic A, Sonnentag O, Lemmetyinen J, Baltzer JL, Kinnard C, Roy A. Reviews and syntheses: recent advances in microwave remote sensing in support of terrestrial carbon cycle science in Arctic–boreal regions. Biogeosciences. 2023;20(14):2941–70. https://doi.org/10.5194/bg-20-2941-2023.
31. McRoberts RE, Holden GR, Nelson MD, Liknes GC, Gormanson DD. Using satellite imagery as ancillary data for increasing the precision of estimates for the forest inventory and analysis program of the USDA forest service. Can J For Res. 2005;35(12):2968–80. https://doi.org/10.1139/x05-222.

32. Mohammed Khan A, Kuri A, Ahammed S, Al Muqtadir Abir K, Arfin-Khan MA. A google earth engine approach for anthropogenic forest fire assessment with remote sensing data in Rema-Kalenga wildlife sanctuary, Bangladesh. Geol Ecol Landsc. 2023;9:45. https://doi.org/10.1080/24749508.2023.2165297.
33. Montgomery DC, Peck EA, Vining GG. Introduction to linear regression analysis. Hoboken: John Wiley & Sons; 2021.
34. Mukul SA, Saha N. Conservation benefits of tropical multifunctional land-uses in and around a forest protected area of Bangladesh. Land. 2017;6(1):2. https://doi.org/10.3390/land6010002.
35. Næsset E. Predicting forest stand characteristics with airborne scanning laser using a practical two-stage procedure and field data. Remote Sens Environ. 2002;80:88–99. https://doi.org/10.1016/S0034-4257(01)00290-5.
36. Næsset E. Practical large-scale forest stand inventory using a small-footprint airborne scanning laser. Scand J For Res. 2004;19:164–79. https://doi.org/10.1080/02827580310019257.
37. Næsset E. Airborne laser scanning as a method in operational forest inventory: status of accuracy assessments accomplished in Scandinavia. Scand J For Res. 2007;22(5):433–42. https://doi.org/10.1080/02827580701672147.
38. Næsset E, Ørka HO, Solberg S, Bollandsås OM, Hansen EH, Mauya E, Zahabu E, et al. Mapping and Estimating forest area and aboveground biomass in Miombo Woodlands in Tanzania Using Data from Airborne Laser Scanning, TanDEM-X, RapidEye, and Global Forest Maps: a comparison of estimated precision. Remote Sens Environ. 2016;175:282–300. https://doi.org/10.1016/j.rse.2016.01.006.
39. Niu J, Mao C, Xiang J. Based on ecological footprint and ecosystem service value, research on ecological compensation in Anhui Province China. Ecol Indicat. 2024;158:111341. https://doi.org/10.1016/j.ecolind.2023.111341.
40. Packale´n P, Mehta ¨talo L, Maltamo M. ALS-based estimation of plot volume and site index in a eucalyptus plantation with a nonlinear mixed-effect model that accounts for the clone effect. Ann For Sci. 2011;68:1085–92. https://doi.org/10.1007/s13595-011-0124-9.
41. Peña-Lara VA, Dupuy JM, Reyes-Garcia C, Sanaphre-Villanueva L, Portillo-Quintero CA, Hernández-Stefanoni JL. Modelling species richness and functional diversity in tropical dry forests using multispectral remotely sensed and topographic data. Remote Sens. 2022;14(23):5919. https://doi.org/10.3390/rs14235919.
42. R Core Team. R foundation for statistical computing. R: a language and environment for statistical computing. Vienna: R Core Team; 2019.
43. Purdy AJ, Fisher JB, Goulden ML, Colliander A, Halverson G, Tu K, Famiglietti JS. SMAP soil moisture improves global evapotranspiration. Remote Sens Environ. 2018;219:1–14. https://doi.org/10.1016/j.rse.2018.09.023.
44. Ramachandra T, Soman D, Naik AD, Chandran MSJJ. Appraisal of forest ecosystems goods and services: challenges and opportunities for conservation. J Biodivers. 2017;8(1):12–33. https://doi.org/10.1080/09766901.2017.1346160.
45. Rana P, Popescu S, Tolvanen A, Gautam B, Srinivasan S, Tokola T. Estimation of tropical forest aboveground biomass in Nepal using multiple remotely sensed data and deep learning. Int J Remote Sens. 2023;44(17):5147–71. https://doi.org/10.1080/01431161.2023.2240508.
46. Rana P, Vauhkonen J. Stochastic multicriteria acceptability analysis as a forest management priority mapping approach based on airborne laser scanning and field inventory data. Landsc Urban Plan. 2023;230:104637.
47. Rana P, Vauhkonen J, Junttila V, Hou Z, Gautam B, Cawkwell F, Tokola T. Large tree diameter distribution modelling using sparse airborne laser scanning data in a subtropical forest in Nepal. ISPRS J Photogramm Remote Sens. 2017;134:86–95.
48. Rana P, Gautam B, Tokola T. Optimizing the number of training areas for modeling above-ground biomass with ALS and multispectral remote sensing in subtropical Nepal. Int J Appl Earth Obs Geoinf. 2016;49:52–62.
49. Rana P, Korhonen L, Gautam B, Tokola T. Effect of field plot location on estimating tropical forest above-ground biomass in Nepal using airborne laser scanning data. ISPRS J Photogramm Remote Sens. 2014;94:55–62.
50. Rana MP, Sohel MSI, Mukul SA, Chowdhury MSH, Akhter S, Koike M. Implications of ecotourism development in protected areas: a study from Rema-Kalenga Wildlife Sanctuary Bangladesh. iForest. 2010;3:23–9. https://doi.org/10.3832/ifor0520-003.
51. Rexhepi BR, Rexhepi FG, Sadiku MK, Dauti B. Ecosystem services of forests and their economic valuation: prospects for sustainable development. Sci J Ukr J For Wood Sci. 2024. https://doi.org/10.3154/forest/1.2024.109.
52. Redowan M, Akter S, Islam N. Analysis of forest cover change at Khadimnagar National Park, Sylhet, Bangladesh, using Landsat TM and GIS data. J For Res. 2014;25:393–400. https://doi.org/10.1007/s11676-014-0467-9.
53. Sohel MSI, Rana MP, Alam M, Akhter S, Alamgir M. The carbon sequestration potential of forestry sector: Bangladesh context. J For Environ Sci. 2009;25(3):157–65.
54. Saatchi SS, Harris NL, Brown S, Lefsky M, Mitchard ET, Salas W, Morel A. Benchmark map of forest carbon stocks in tropical regions across three continents. Proc Natl Acad Sci. 2011;108(24):9899–904. https://doi.org/10.1073/pnas.1019576108.
55. Rodriguez-Galiano VF, Ghimire B, Rogan J, Chica-Olmo M, Rigol-Sanchez JP. An assessment of the effectiveness of a random forest classifier for land-cover classification. ISPRS J Photogramm Remote Sens. 2012;67:93–104. https://doi.org/10.1016/j.isprsjprs.2011.11.002.
56. Simard M, Pinto N, Fisher JB, Baccini A. Mapping forest canopy height globally with spaceborne lidar. J Geophys Res Biogeosci. 2011. https://doi.org/10.1029/2011JG001708.
57. Shamsoddini A, Trinder JC, Turner R. Pine plantation structure mapping using WorldView-2 multispectral image. Int J Remote Sens. 2013;34:3986–4007. https://doi.org/10.1080/01431161.2013.772308.
58. Silveira EMDO, Cunha LIF, Galvão LS, Withey KD, Acerbi Júnior FW, Scolforo JRS. Modelling aboveground biomass in forest remnants of the Brazilian Atlantic Forest using remote sensing, environmental and terrain-related data. Geocarto Int. 2021;36(3):281–98. https://doi.org/10.1080/10106049.2019.1594394.
59. Silveira EM, Radeloff VC, Martinuzzi S, Pastur GJM, Bono J, Politi N, Pidgeon AM. Nationwide native forest structure maps for Argentina based on forest inventory data, SAR Sentinel-1 and vegetation metrics from Sentinel-2 imagery. Remote Sens Environ. 2023;285:113391. https://doi.org/10.1016/j.rse.2022.113391.
60. Zheng G, Yang Y, Yang D, Dafflon B, Lei H, Yang H. Satellite-based simulation of soil freezing/thawing processes in the northeast Tibetan Plateau. Remote Sens Environ. 2019;231:111269. https://doi.org/10.1016/j.rse.2019.111269.
61. Zheng D, Heath LS, Ducey MJ. Forest biomass estimated from MODIS and FIA data in the Lake States: MN, WI and MI, USA. Forestry. 2007;80(3):265–78. https://doi.org/10.1093/forestry/cpm015.

62. Zhu XX, Tuia D, Mou L, Xia GS, Zhang L, Xu F, Fraundorfer F. Deep learning in remote sensing: a comprehensive review and list of resources. IEEE Geosci Remote Sens Mag. 2017;5(4):8–36. https://doi.org/10.1109/MGRS.2017.2762307.
63. Zhu Y, Feng Z, Lu J, Liu J. Estimation of forest biomass in Beijing (China) using multisource remote sensing and forest inventory data. Forests. 2020;11(2):163. https://doi.org/10.3390/f11020163.